International Journal of Heat and Mass Transfer 52 (2009) 1817–1826

Contents lists available at ScienceDirect

International Journal of Heat and Mass Transfer

journal homepage: www.elsevier.com/locate/ijhmt

Unsteady conjugate forced convection heat/mass transfer in ensembles of spherical particles with cell models

Gheorghe Juncu *

Politehnica University Bucharest, Catedra Inginerie Chimica, Polizu 1, 011061 Bucharest, Romania

ARTICLE INFO

Article history:
Received 15 August 2008
Available online 6 December 2008

Keywords:
Conjugate heat transfer
External flow
Forced convection
Ensembles
Sphere
Cell models

ABSTRACT

Numerical methods are used to investigate the transient, conjugate, forced convection heat/mass transfer in multiparticle systems at low to moderate Reynolds numbers. The interparticle interactions have been accounted for by using the simple cell models. The momentum and heat/mass balance equations were solved numerically in spherical coordinates system by a finite difference method. The values considered for the sphere Reynolds number are $Re < 100$. The computations were focused on the influence of the voidage and physical properties ratios on the heat/mass transfer rate for sphere Peclet number, $10 \leqslant Pe \leqslant 1000$.

1. Introduction

When Perelman [1] investigated the forced convective heat transfer in a boundary-layer flow over an internally heated semi-infinite flat plate with two-dimensional thermal conduction and interface temperature unknown, he used for the first time the words conjugate heat transfer. For bodies with spherical symmetry, the first conjugate heat/mass transfer studies are [2–4]. Using the boundary-layer formalism, only the case of fluid spheres with internal circulation at high Peclet numbers was considered. It must be mentioned that the boundary-layer approximation used in [2–4] is not entirely similar to that employed for the flat plate [1,5–10]. For fluid spheres with internal circulation at high Pe numbers, thin thermal/concentration boundary layers on both sides of the interface were considered. However, the assumption of infinite sphere practiced in [2–4], (assumption necessary to justify the similarity transformations inside the sphere) is a questionable one. In spite of this fact, the boundary-layer approximation was recently used to analysed the conjugate heat/mass transfer from a sphere in [11–13].

Brounshtein et al. [14] proposed a different approach. The heat/mass transfer inside the sphere is described by the usual balance equations (the Kronig–Brink model was used in [14] for circulating spheres at high Pe numbers), but the boundary condition at the interface takes into consideration the resistance of the continuous phase. The external heat/mass transfer coefficient is assumed to be known and equal to its steady value (the values used are those calculated for the heat/mass transfer from a sphere with constant temperature/concentration).

For motionless systems, the unsteady conjugate heat/mass transfer from a sphere was studied in [15–19]. The first numerical solution for the unsteady, conjugate, forced convection heat transfer from a rigid sphere to an ambient fluid flow was obtained by Brauer [20]. For values of the thermal diffusivity ratio greater or equal to 1, Brauer [20] showed that the volume heat capacity ratio has a distinct influence on the heat transfer rate and proposed an analogy criterion between the unsteady conjugate heat and mass transfer. Abtramzon and Borde [21] gave a numerical solution of the conjugate problem for the case of equal thermal conductivities and volume heat capacities of the two phases. Baboolal et al. [22] investigated the conjugate mass transfer of SO_2 from air to water drops. The interface boundary conditions used in [22] are not the standard interface boundary conditions employed in conjugate transfer studies. Oliver and Chung [23] analysed the unsteady conjugate heat transfer from a spherical droplet or particle in creeping flow considering the thermal diffusivities ratio equal to 1 and the volumetric heat capacities ratio varying between 0.333 and 3. For Henry number equal to 1, the influence of the diffusivities ratio on the unsteady conjugate mass transfer from a drop in creeping flow was studied in [24]. In the manner of Oliver and Chung [23], other cases were analysed in [25–29]. For values of the thermal conductivity and volume heat capacity ratios varying between 0.01 and 100, it was shown in [30–33] that, for given Pe number, both the fractional and overall asymptotic *Nu* numbers depend on two parameters: thermal conductivity and volume heat

* Tel./fax: +40 21 345 0596.
E-mail addresses: juncugh@netscape.net, juncu@easynet.ro

0017-9310/$ - see front matter © 2008 Elsevier Ltd. All rights reserved.
doi:10.1016/j.ijheatmasstransfer.2008.10.010

List of symbols

a	radius of the sphere
b	radius of the fluid envelope
c_P	heat capacity
C	concentration
C_D	total drag coefficient
C_{DF}	friction drag coefficient
C_{DP}	pressure drag coefficient
d	diameter of the sphere, $d = 2\ a$
f	friction factor
k	thermal conductivity
Nu	instantaneous overall Nusselt number
Nu_θ	instantaneous local Nusselt number
Pe	Peclet number, $Pe = Re\ Pr$
Pr	Prandtl (Schmidt) number, $Pr = \nu/\alpha_f$
r	dimensionless radial coordinate, r^*/a, in spherical coordinate system
r^*	radial coordinate in spherical coordinate system
Re	Reynolds number based on the diameter of the sphere, $Re = U_0 d/\nu$
t	time
T	temperature
U_0	superficial velocity
V_R	dimensionless radial velocity component
V_θ	dimensionless tangential velocity component
Z	dimensionless temperature defined by the relation, $Z_{(p)} = \frac{T_{f(p)} - T_{f,0}}{T_{p,0} - T_{f,0}}$

Greek symbols

α	thermal diffusivity
γ	dimensionless cell boundary, $\gamma = b/a$
ϵ	voidage
Φ	conductivity ratio, k_p/k_f
ν	kinematic viscosity
θ	polar angle in spherical coordinate system
ρ	density
$\tau_{(p)}$	dimensionless time or Fourier number, $\tau = 4\ t\ \alpha_{f\ (p)}/d^2$
ω	dimensionless vorticity
ψ	dimensionless stream function
Ξ	volume heat capacity ratio, $(\rho_p\ c_{P,p})/(\rho_f\ c_{P,f})$

Subscripts

f	refers to the fluid
p	refers to particle (sphere)
s	refers to the surface of the sphere
0	initial conditions

capacity ratios. This dependence is complex and does not allow simple approximations. An analogy criterion, equivalent to that proposed in [20], between the unsteady conjugate heat and mass transfer was derived in [33]. For some specific cases, numerical solutions of the unsteady conjugate heat/mass transfer from a sphere were obtained in [34–42]. Paschedag et al. [42] have shown that, for large Pe numbers, the concentration pattern inside the sphere follows the Kronig–Brink model. The unsteady conjugate mass transfer from a sphere in the presence of a chemical reaction was analysed in [43–47]. The influence of the Marangoni convection on the unsteady conjugate mass transfer from a drop was recently investigated in [48].

It is readily conceded that, in most real life problems, one often encounters ensembles of spherical particles rather than a single sphere. The sphere-in-cell geometry has been widely used as a simple model for the representation of ensembles of spherical particles. In spite of its highly idealized nature, the cell-model offers a reasonable approach at least for macroscopic transport parameters.

The convective heat/mass transfer in cell models was analysed in few articles [31,49–56] (here we refer only to non-circulating spheres). Except for [31] and [56], in all the other articles the temperature/concentration inside the sphere were considered spatially uniform and constant in time. In [31], only some cases of unsteady conjugate heat transfer for very low Pe numbers were investigated. The steady-state solutions for the catalytic reaction were obtained in [56].

The aim of this paper is to analyse the unsteady conjugate heat/mass transfer in an ensemble of spherical particles modeled by the sphere-in-cell geometry. To our knowledge, this problem was not investigated until now. The influence of the physical properties ratio and voidage on the heat/mass transfer rate is investigated for $Re < 100$ (Re is the sphere Reynolds number) and $10 \leqslant Pe \leqslant 1000$.

2. Model equations

Consider the steady, axisymmetric flow of a Newtonian incompressible fluid with a superficial velocity U_0 and concentration/temperature $C_{f,0}/T_{f,0}$ past an assemblage of spheres. The initial concentration/temperature of the particles, $C_{p,0}/T_{p,0}$, are different from that of the main stream.

The main problem in modeling of such systems is that of particle–particle interactions. The cell-models replace the difficult many-body problem by a simple and conceptually more attractive one involving only one sphere. Wall effects and/or entry and exit effects are neglected. The assembly of particles in the fluid is assumed to be uniform and each sphere is fixed in space. The interaction of each sphere with its neighbors is modeled by a hypothetical spherical envelope of fluid of radius b. The size of the cell (envelope) is given by the voidage of the assemblage, ε, as:

$$\frac{b}{a} = \gamma = (1-\varepsilon)^{-1/3}$$

where a is the radius of the sphere.

To define the mathematical model of the present problem, we consider valid the following statements:

- during the heat/mass transfer process, the volume and shape of the sphere remain constant;
- the effects of buoyancy and viscous dissipation are negligible (the dissipation function becomes important in high-speed flows, i.e. flows with large velocity gradients, and in flows of fluids with extremely large viscosities; this is not the case with the present problem);
- the physical properties of the sphere and the fluid are considered to be uniform, isotropic and constant;
- no emission or absorption of radiant energy;
- no phase change;
- no chemical reaction inside the sphere or in the surrounding fluid.

The assumptions practiced in this work are those usually employed in the analysis of the analogy between heat and mass transfer. For the simplicity and clarity of the presentation, in the remainder of this work, we will use only the terminology specific to heat transfer.

Non-dimensionalizing the basic conservation balances for momentum and thermal energy using the free stream fluid properties and the sphere radius, we obtain the governing differential equations:

– fluid motion

$$E^2(\psi) = \omega r \sin\theta \tag{1a}$$

$$\frac{Re}{2}\left[\frac{\partial\psi}{\partial r}\frac{\partial}{\partial\theta}\left(\frac{\omega}{r\sin\theta}\right) - \frac{\partial\psi}{\partial\theta}\frac{\partial}{\partial r}\left(\frac{\omega}{r\sin\theta}\right)\right]\sin\theta = E^2(\omega r\sin\theta) \tag{1b}$$

– energy

$$\frac{\partial Z}{\partial\tau} + \frac{RePr}{2}\left(V_R\frac{\partial Z}{\partial r} + \frac{V_\theta}{r}\frac{\partial Z}{\partial\theta}\right) = \Delta Z \tag{2a}$$

$$\frac{\partial Z_p}{\partial\tau_p} = \Delta Z_p \tag{2b}$$

where

$$E^2 = \frac{\partial^2}{\partial r^2} + \frac{\sin\theta}{r^2}\frac{\partial}{\partial\theta}\left(\frac{1}{\sin\theta}\frac{\partial}{\partial\theta}\right),$$

$$\Delta = \frac{1}{r^2}\frac{\partial}{\partial r}\left(r^2\frac{\partial}{\partial r}\right) + \frac{1}{r^2\sin\theta}\frac{\partial}{\partial\theta}\left(\sin\theta\frac{\partial}{\partial\theta}\right)$$

$$V_R = -\frac{1}{r^2\sin\theta}\frac{\partial\psi}{\partial\theta}, V_\theta = \frac{1}{r\sin\theta}\frac{\partial\psi}{\partial r}$$

$$Re = \frac{U_0 d}{\nu}, Pr = \frac{\nu}{\alpha_f}.$$

The boundary conditions are:

– axis of symmetry, $\theta = 0, \pi$

$$\psi = \omega = \frac{\partial Z}{\partial\theta} = \frac{\partial Z_p}{\partial\theta} = 0, \tag{3a}$$

– surface of the sphere, $r = 1$,

$$\psi = 0, Z = Z_p, \Phi\frac{\partial Z_p}{\partial r} = \frac{\partial Z}{\partial r}, \tag{3b}$$

– center of the sphere, $r = 0$

$$Z_p = \text{finite}, \tag{3c}$$

– cell boundary, $r = \gamma$

$$\psi = 1/2r^2\sin^2\theta, \quad \omega = 2\frac{V_\theta - \sin\theta}{r}(\text{Happel,[57]}) \text{ or}$$
$$\omega = 0(\text{Kubawara,[58]}), Z = 0. \tag{3d}$$

The dimensionless initial conditions are:

$$\tau = \tau_p = 0, \quad Z_p = 1, \quad Z = 0. \tag{4}$$

The physical quantities of interest are the dimensionless sphere average temperature$\bar{Z}_p$, the local Nusselt number, Nu_θ, the overall Nusselt number, $Nu_{(p)}$ and the fractional Nusselt numbers, Nu_{int}, Nu_{ext}. Considering as driving force the difference between the instantaneous sphere average temperature and the free stream temperature, the local and overall Nu numbers are given by:

$$Nu_\theta = -\frac{2}{\bar{Z}_p}\frac{\partial Z}{\partial r}|_{r=1-} \text{ or } \left(Nu_\theta = -\Phi\frac{2}{\bar{Z}_p}\frac{\partial Z}{\partial r}\Big|_{r=1+}\right), \quad \text{if} \quad \Phi < 1,$$

$$Nu_\theta = -\frac{2}{\bar{Z}_p}\frac{\partial Z}{\partial r}\Big|_{r=1+}, \quad \text{if} \quad \Phi \geq 1 \tag{5a}$$

$$Nu = -\Phi\frac{1}{\bar{Z}_p}\int_0^\pi \frac{\partial Z}{\partial r}\Big|_{r=1+}\sin\theta d\theta, \quad \text{if} \quad \Phi \leq 1$$

$$Nu = -\frac{1}{\bar{Z}_p}\int_0^\pi \frac{\partial Z}{\partial r}\Big|_{r=1+}\sin\theta d\theta, \quad \text{if} \quad \Phi > 1 \tag{6a}$$

or

$$Nu = -\frac{2}{3}\frac{d\ln\bar{Z}_p}{d\tau_p}, \quad \text{if} \quad \Phi \leq 1.$$

$$Nu = -\Xi\frac{2}{3}\frac{d\ln\bar{Z}_p}{d\tau_p}, \quad \text{if} \quad \Phi > 1. \tag{6b}$$

The sphere average temperature was calculated with the relation,

$$\bar{Z}_p = \frac{3}{2}\int_0^1\int_0^\pi Z_p r^2\sin\theta d\theta dr. \tag{7}$$

The fractional Nusselt numbers were computed as:

$$Nu_{\text{int}} = -\frac{1}{\bar{Z}_p - \bar{Z}_{p,s}}\int_0^\pi \frac{\partial Z}{\partial r}\Big|_{r=1+}\sin\theta d\theta, \tag{8a}$$

$$Nu_{\text{ext}} = -\frac{1}{\bar{Z}_{p,s}}\int_0^\pi \frac{\partial Z}{\partial r}\Big|_{r=1+}\sin\theta d\theta, \tag{8b}$$

where $\bar{Z}_{p,s}$ is the dimensionless surface average temperature of the sphere,

$$\bar{Z}_{p,s} = \frac{1}{2}\int_0^\pi Z_p|_{r=1}\sin\theta d\theta. \tag{9}$$

The relation between the fractional and overall Nu numbers is:

$$\frac{1}{Nu} = \frac{1}{Nu_{\text{int}}} + \Phi\frac{1}{Nu_{\text{ext}}} \quad \text{if} \quad \Phi \leq 1,$$

$$\frac{1}{Nu} = \frac{1}{\Phi}\frac{1}{Nu_{\text{int}}} + \frac{1}{Nu_{\text{ext}}} \quad \text{if} \quad \Phi \geq 1.$$

3. Method of solution

The energy balance equations and the Navier–Stokes equations were solved numerically. The Navier–Stokes equations being uncoupled from the energy balance equations can be solved independently of them. The algorithm employed is the nested defect-correction iteration, [59,60]. Eq. (1a) was discretized with the central second-order accurate finite difference scheme. A double discretization (upwind and central finite difference schemes), necessary for the defect-correction iteration, was used for Eq. (1b). The numerical solutions were calculated on a mesh with the discretization steps $\Delta\theta = \pi/512$ and $\Delta r = 1/512$.

The boundary conditions [Eq. (3b)] for the dimensionless temperature show that the interface between the two media is not a *surface of discontinuity* [61] or, in other words, we have an *ideal contact* between the two phases [62]. The numerical technique used to solve the heat balance equations, under the conditions mentioned previously, consists of:

- the Eqs. (2a), (2b) are rewritten as a single equation with discontinuous coefficients (the existence of the solutions for equations with discontinuous coefficients was proved in [63,64]);
- the spatial discretization of the equation with discontinuous coefficients with *conservative finite difference schemes* [62,65] or *control volume schemes* [66];
- the discrete parabolic equation was solved by the implicit ADI method.

In order to obtain a positive definite discrete operator (the continuous operator is positive definite, [62]), for $r > 1$, a regularized scheme, with the regularization coefficient given in [67], was used. For $r < 1$, the discrete operator is identical to that provided by the

standard central order scheme. Numerical experiments were made on grids with the discretization steps $\Delta\theta = \pi/64$, $\pi/128$, $\pi/256$, $\pi/512$ and $\Delta r = 1/64$, $1/128$, $1/256$, $1/512$. The solutions obtained on the grid with $\Delta\theta = \pi/256$ and $\Delta r = 1/256$ may be considered mesh-independent. For this reason, the heat transfer results presented in the next section were computed on the mesh with $\Delta\theta = \pi/256$ and $\Delta r = 1/256$. The time step was variable and changed from the start of the computation to the final stage. The initial and final values of the time step depend on the parameter values.

4. Results

The cell models describe appropriately the hydrodynamics of the ensembles of rigid spheres for particle Reynolds numbers not exceeding ≈100. The values considered for the Prandtl number are, $Pr \geqslant 1$, with the mention that $10 \leqslant Pe = Re\,Pr \leqslant 1000$. We consider $Pe = 10$ as lower limit due to the discussions, for low values of the Peclet number, about the boundary condition for the dimensionless temperature at $r = \gamma$ [31,55]. To have a rigorous control over the numerical errors, the maximum value for the Peclet number was 1000. The conductivity ratio, Φ, and the volume heat capacity ratio, Ξ, take values in the range 10^{-2} to 10^{2}. The values considered for the dimensionless cell boundary, γ, are: $\gamma = 1.168$, 1.25, 1.5, 2, 3. The voidage values corresponding to these γ values are, $\varepsilon = 0.372$, 0.488, 0.704, 0.875, 0.963. The present values of the dimensionless cell boundary are similar to those used in [49]. All the computations were made using both cell-models, i.e. Happel [57] and Kubawara [58].

The numerical values of the drag coefficients and friction factor calculated in the present work for $Re \leqslant 50$ are presented in Table 1. The total drag coefficient was calculated with the relation:

$$C_D = \int_0^{\pi} C_P(\theta) \sin 2\theta d\theta + \frac{8}{Re} \int_0^{\pi} \omega_s \sin^2 \theta d\theta, \tag{10}$$

where the pressure coefficients $C_P(\theta)$ on the surface of the sphere was computed with the relation,

$$C_P(\theta) = \frac{4}{Re} \int_0^{\theta} \left(\left.\frac{\partial \omega}{\partial r}\right|_{r=1} + \omega_s \right) d\theta.$$

The two integrals in (10) are referred as the pressure and friction drag coefficients and are denoted C_{DP} and C_{DF}, respectively. The friction factor, f, was calculated with the relation:

$$f = \frac{3}{4} C_D \varepsilon^3$$

For the same Re values and similar ε values, the results presented in Table 1 agree well with those obtained in [68,69].

The Navier–Stokes equations were also solved numerically for $Re = 100$. The results obtained are presented separately in Table 2. We observe that: (i) the drag coefficients decrease with the increase in ε; (ii) the friction factor does not decrease with the increase in ε. The same results may be obtained from the values of the drag coefficients presented in [69]. This aspect contradicts

Table 1
Values of the drag coefficients and friction factor.

Re	γ	ε	Cell model							
			Happel				Kubawara			
			C_{DP}	C_{DF}	C_D	f	C_{DP}	C_{DF}	C_D	f
0.1	1.168	0.372	19043.5	7240.0	26283.5	1017.8	23394.8	7725.6	31120.4	1205.1
	1.25	0.488	6292.57	3661.87	9954.44	867.74	8273.17	3989.54	12262.7	1068.83
	1.5	0.704	1112.97	1266	2378.97	622.54	1618.08	1429.97	3048.05	797.63
	2	0.875	319.999	551.118	871.117	437.64	450.7	630.99	1081.69	543.49
	3	0.963	161.1	315.67	476.77	319.34	196.74	352.78	549.52	368.06
1	1.168	0.372	1904.5	724.0	2628.5	101.8	2339.7	772.57	3112.18	120.51
	1.25	0.488	629.36	366.2	995.56	86.77	827.43	398.97	1226.40	106.89
	1.5	0.704	111.39	126.63	238.01	62.204	161.90	143.02	304.92	79.69
	2	0.875	32.11	55.17	87.28	43.85	45.18	63.15	108.33	54.43
	3	0.963	16.28	31.72	47.99	32.15	19.82	35.41	55.23	36.99
10	1.168	0.372	191.65	72.52	264.16	10.23	235.28	77.38	312.66	12.11
	1.25	0.488	63.92	36.76	100.68	8.78	83.83	40.05	123.88	10.80
	1.5	0.704	11.97	12.90	24.86	6.498	17.08	14.55	31.63	8.27
	2	0.875	4.06	5.96	10.03	5.04	5.35	6.74	12.09	6.05
	3	0.963	2.48	3.91	6.396	4.28	2.78	4.20	6.98	4.68
50	1.168	0.372	43.33	14.98	58.31	2.26	52.52	15.99	68.51	2.65
	1.25	0.488	16.40	7.86	24.26	2.12	20.75	8.56	29.31	2.56
	1.5	0.704	4.41	3.12	7.53	1.97	5.63	3.48	9.11	2.38
	2	0.875	1.95	1.70	3.65	1.83	2.29	1.87	4.16	2.09
	3	0.963	1.25	1.24	2.48	1.66	1.34	1.30	2.63	1.76

Table 2
Values of the drag coefficients and friction factor for $Re = 100$.

Re	γ	ε	Cell model							
			Happel				Kubawara			
			C_{DP}	C_{DF}	C_D	f	C_{DP}	C_{DF}	C_D	f
100	1.168	0.372	27.22	8.01	35.22	1.364	32.33	8.56	40.89	1.583
	1.25	0.488	11.47	4.37	15.84	1.380	14.03	4.765	18.795	1.638
	1.5	0.704	3.438	1.847	5.285	1.381	4.243	2.064	6.308	1.649
	2	0.875	1.583	1.054	2.637	1.325	1.832	1.156	2.988	1.50
	3	0.963	1.048	0.784	1.832	1.227	1.117	0.819	1.936	1.297

Table 3
Comparison of the present *Nu* values with previous studies for spheres with constant temperature in creeping flow.

γ	ε	*Pe*	*Nu*	
			Present	Pfeffer and Happel [47]
1.25	0.488	1	10.01	10.00
		5	10.03	10.02
		10	10.03	10.07
		50	11.30	11.34
		100	13.97	13.52
2	0.875	1	3.99	4.01
		5	4.03	4.12
		10	4.34	4.40
		50	6.48	6.47
3	0.963	1	2.95	3.02
		5	3.26	3.30
		10	3.75	3.75
		50	5.59	5.59

the experimental data and correlations (Ergun type relations). The idea, [51], *that one consider cells whose volume is constant but whose shape is a function of the Reynolds number* is difficult to implement numerically.

For this reason, the maximum *Re* value considered in this work is, *Re* = 50. The heat transfer results obtained for *Re* = 100 are not presented. We consider that discussions about heat transfer results calculated with questionable hydrodynamic data should be avoided. However, it must be mentioned that the heat transfer data obtained for *Re* = 100 do not change the results of the present work.

There are no data in literature to verify the accuracy of the present heat transfer computations. The simulation of the case of sphere with constant temperature can be viewed as a partial validation of the present computation. Table 3 shows a very good agreement between the present computations and the values obtained in [49]. For large *Pe* numbers, in creeping flow, the relation derived by Pfeffer [50] provides the following results (Pfeffer [50] solved the concentration boundary-layer equation in creeping flow): Nu ($Pe = 1000$, $\varepsilon = 0.372$) = 37.10, Nu ($Pe = 1000$, $\varepsilon = 0.488$) = 28.39, Nu ($Pe = 1000$, $\varepsilon = 0.704$) = 19.93. These values agree very well with the present calculations for *Pe* = 1000 and creeping flow (see Table 6).

For given *Re*, *Pe* and ε values, the influence of the conductivity and heat capacity ratios on the asymptotic *Nu* values is similar to that observed for a single sphere [30–33]. The decrease in ε decreases the effect of Ξ but even for small voidage values the effect of the volume heat capacity ratio cannot be considered negligible. The thermal wake phenomenon is present. A sample from our numerical simulations is presented in Table 4 and Fig. 1. Fig. 2a plots the asymptotic values of the local *Nu* number for $\Xi = 1$. In comparison, Fig. 2b depicts the asymptotic values of the local *Nu* number for the single sphere. The results presented in Table 4 and Figs. 1 and 2a were obtained using Happel model. The Kubawara model provides similar results. The first row in Table 4, i.e. the row corresponding to $\Phi = 0$, presents the numerical results obtained for the internal problem, i.e. the unsteady heat transfer

Table 4
Asymptotic values of the overall and fractional *Nu* numbers for *Re* = 1,*Pe* = 100 and $\gamma = 1.25$.

Φ	Ξ								
	0.01	0.1	0.2	0.5	1	2	5	10	100
0	6.56								
0.01	6.56[a]	6.56	6.56	6.56	6.56	6.56	6.56	6.56	6.56
	6.59[b]	6.59	6.59	6.59	6.59	6.59	6.59	6.59	6.59
	13.28[c]	14.23	14.28	14.32	14.33	14.33	14.34	14.34	14.34
0.1	5.99[*]	6.38	6.39	6.40	6.40	6.40	6.40	6.40	6.40
	6.96	6.71	6.70	6.70	6.70	6.70	6.70	6.70	6.70
	4.26	13.32	13.84	14.15	14.25	14.30	14.33	14.33	14.35
0.2	3.90[*]	6.16	6.19	6.21	6.22	6.22	6.22	6.22	6.22
	8.18	6.84	6.83	6.82	6.81	6.81	6.81	6.81	6.81
	1.50	12.38	13.38	13.98	14.17	14.27	14.33	14.35	14.35
0.5	1.64[*]	5.37	5.57	5.66	5.68	5.70	5.71	5.71	5.71
	9.28	7.33	7.21	7.16	7.14	7.13	7.13	7.12	7.12
	1.00	10.04	12.18	13.52	13.97	14.19	14.32	14.36	14.41
1	0.8[*]	3.99[*]	4.53	4.80	4.89	4.93	4.95	4.96	4.96
	9.66	8.1	7.81	7.65	7.60	7.58	7.57	7.56	7.56
	0.9	7.87	10.79	12.92	13.68	14.06	14.29	14.37	14.43
2	0.5[*]	4.71	6.07	7.04	7.36	7.52	7.61	7.64	7.67
	9.89	8.93	8.59	8.35	8.26	8.22	8.20	8.19	8.18
	0.5	6.40	9.40	12.18	13.28	13.86	14.21	14.33	14.43
5	0.7[*]	4.83	6.92	9.01	9.88	10.35	10.64	10.74	10.83
	9.94	9.58	9.39	9.19	9.11	9.07	9.04	9.03	9.02
	0.7	5.38	8.13	11.21	12.63	13.42	13.93	14.10	14.26
10	0.66	4.70	6.98	9.58	10.8	11.48	11.92	12.08	12.21
	9.95	9.80	9.70	9.58	9.53	9.49	9.47	9.47	9.46
	0.67	4.94	7.54	10.65	12.18	13.07	13.64	13.84	14.02
100	0.60	4.48	6.97	9.94	11.38	12.33	12.96	13.18	13.38
	9.99	9.98	9.97	9.96	9.95	9.95	9.94	9.94	9.94
	0.60	4.49	7.00	10.05	11.60	12.52	13.15	13.36	13.57
∞	0.587	4.477	6.966	9.993	11.55	12.477	13.09	13.285	13.49

[a] Overall *Nu* number, *Nu*.
[b] Internal *Nu* number, Nu_{int}.
[c] External *Nu* number, Nu_{ext}.
[*] Unfrozen asymptotic values.

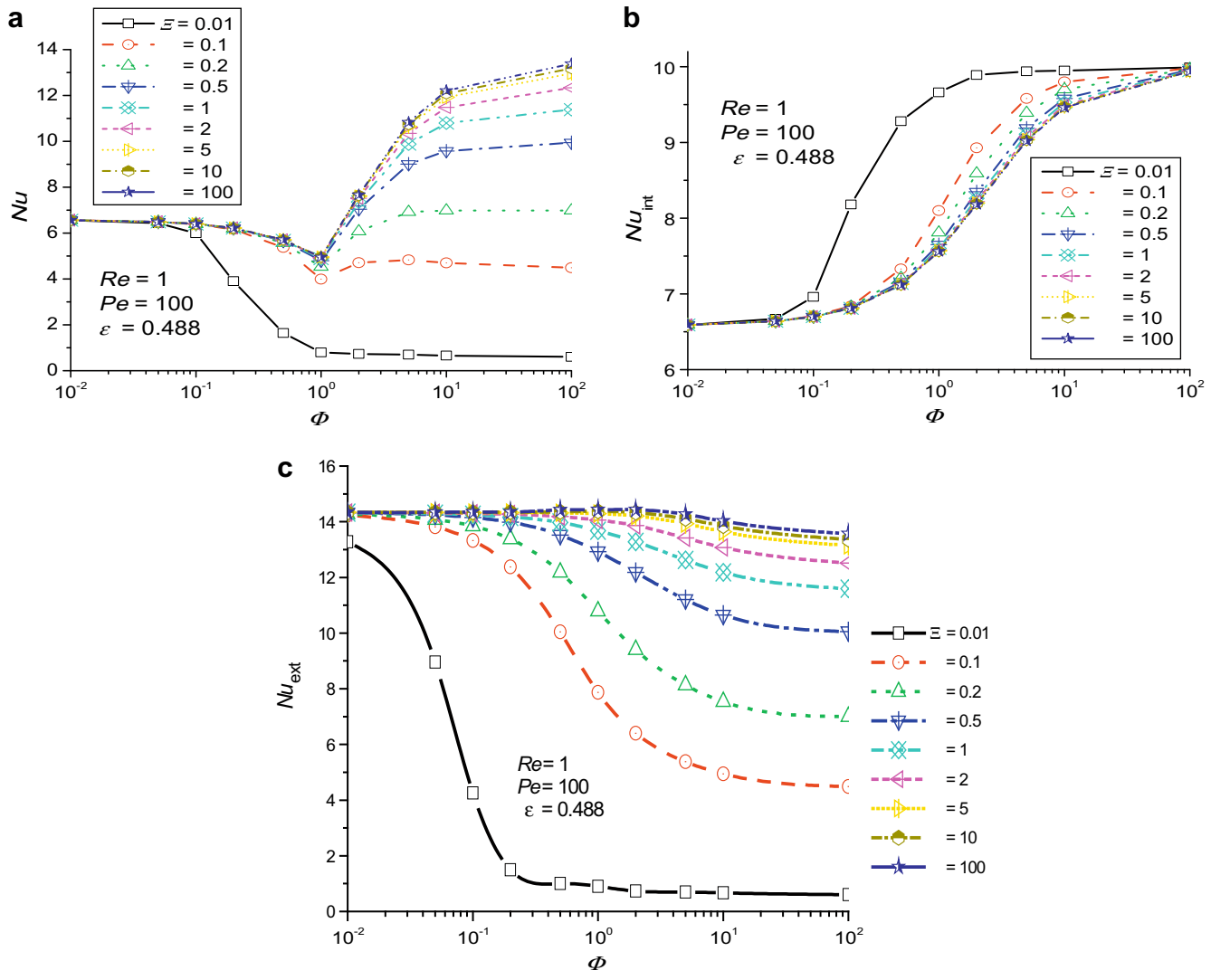

Fig. 1. The influence of the conductivity ratio (Φ) and heat capacity ratio (Ξ) on the asymptotic values of the *Nu* numbers for $Re = 1$, $Pe = 100$ and $\varepsilon = 0.488$; (a) overall *Nu* number; (b) internal *Nu* number; (c) external *Nu* number.

inside a sphere with constant temperature on the surface. The last row in Table 4, i.e. the row corresponding to $\Phi = \infty$, presents the numerical results obtained for the external problem, i.e. the unsteady heat transfer from a sphere with spatially uniform but varying in time temperature. It must be also mentioned that the asymptotic Nu_{int} values varies between the same limits as in the case of the single sphere.

In this work we do not insist on the aspects discussed previously. The present analysis starts from the following observation of Pfeffer [50]: *predictions based upon creeping flow assumption remain accurate for Reynolds number as high as 50*. First, we made numerical simulations with Z_p = constant = 1, keeping *Pe* constant and varying *Re* (this kind of investigation was suggested by [70,71]). The results obtained for $Pe = 100$ and $Pe = 1000$ are presented in Tables 5 and 6. The last row in Tables 5 and 6, i.e. the row corresponding to $\gamma = \infty$ and $\varepsilon = 1$, presents the numerical results obtained for a single sphere. The single sphere results presented in Tables 5 and 6 agree very well with the values calculated in [70,71]. Tables 5 and 6 show that:

- for $\varepsilon = 0.372$, $\varepsilon = 0.488$ and a given *Pe* number, *Nu* may be considered independent from *Re*;
- for $\varepsilon = 0.704$, 0.875, 0.963 and a given *Pe* number, the influence of *Re* on *Nu* increases with the increase in ε;
- the differences between the results provided by Happel and Kubawara models cannot be considered significant;
- for given *Pe* and ε, the influence of *Re* increases with the increase in *Pe*.

For the unsteady conjugate heat transfer, the effect of voidage on the asymptotic *Nu* number values is identical to that observed in Tables 5 and 6. For $\varepsilon = 0.372$, $\varepsilon = 0.488$ and a given *Pe* number, the asymptotic *Nu* values do not depend practically on *Re*. The differences between the asymptotic *Nu* values obtained for different *Re* number and a given *Pe* number are equal to those from Tables 5 and 6.

Fig. 3 plots the asymptotic *Nu* number against the *Pe* number for $\varepsilon = 0.372$ (Fig. 3a), $\varepsilon = 0.488$ (Fig. 3b) and different values of the conductivity and volume heat capacity ratios. The data presented in Fig. 3 were calculated using the Happel model. The Kubawara model gives almost identical results. The curves corresponding to Φ = infinite were obtained by solving the external problem. We depicted the case $Z_p = 1$ because in conjugate heat transfer, the asymptotic *Nu* number tends to *Nu* ($Z_p = 1$) when $\Phi \to \infty$ and

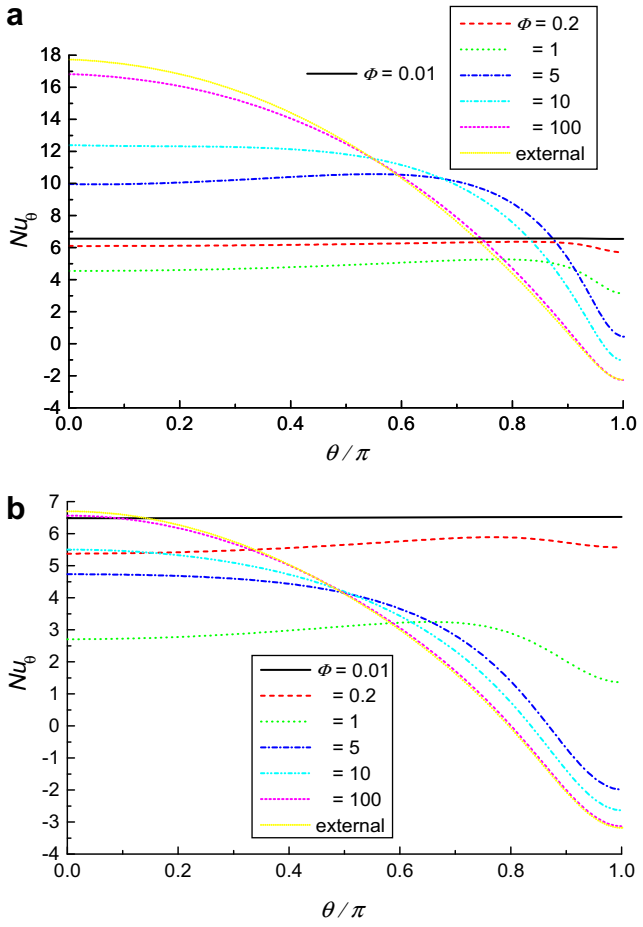

Fig. 2. Asymptotic values of the local *Nu* number for $Re = 1$, $Pe = 100$ and $\Xi = 1$; (a) cell model for $\varepsilon = 0.488$; (b) single sphere.

$\Xi \to \infty$. Fig. 3 shows that Φ and Ξ influence the dependence *Nu* vs. *Pe*. The key parameter, with a strong effect, is the conductivity ratio. For $\Phi = 1$, the influence of *Pe* on the asymptotic *Nu* value is smaller due to the increased contribution of the heat transfer inside the sphere.

A common practice in cell models is to derive heat transfer rate correlations that incorporate the effect of voidage, i.e. *free of voidage correlations*. When the heat transfer rate does not depend explicitly on *Re*, the general form of these correlations is:

$$Nu = g(Pe, \varepsilon) = g_1(Pe)g_2(\varepsilon)$$

For two ε values, ε_1 and ε_2, and a given set of *Pe* values, Pe_k, $k = 1,2,\ldots$, the ratio

$$\frac{Nu_1}{Nu_2} = \frac{g_1(\varepsilon_1)g_2(Pe_k)}{g_1(\varepsilon_2)g_2(Pe_k)} = \frac{g_1(\varepsilon_1)}{g_1(\varepsilon_2)},\ k = 1, 2, \ldots$$

should be constant. For $\varepsilon_1 = 0.488$ and $\varepsilon_2 = 0.372$, this ratio varies in the range (0.72,0.81) (the results obtained for $Z_p = 1$) and in the range (0.68, 0.81) (the results obtained for $\Phi = \infty$, $\Xi = 1$).

Fig. 4 plots the asymptotic *Nu* number against the *Pe* number for $\varepsilon = 0.875$ and $Re = 1$, 10, 50. As comparison criterion, the results obtained for the single spheres and the same *Re*, Φ and Ξ values are depicted in Fig. 5. The data presented in Fig. 4 were calculated using the Happel model. As in the previous cases, the Kubawara model gives almost identical results. The curves corresponding to Φ = infinite were obtained by solving the external problem.

Fig. 4 shows that, for a given *Pe* number, *Re* influences the overall asymptotic *Nu* values. We observe in Fig. 4 that, for a given *Pe* number, the influence of *Re* on asymptotic *Nu* values is significant only for *Re* varying in the range 10–50. Fig. 5 shows that, for the single sphere and a given *Pe* number, the influence of *Re* on asymptotic *Nu* values is also significant for *Re* varying between 1 and 10. As in the previous situation the effect of *Pe* and *Re* on the asymptotic *Nu* values depends on the value of the conductivity ratio. For $\Phi = 1$ and a given *Pe* number, in both cases (the cell model and the single sphere), the influence of *Re* on overall asymptotic *Nu* values is less significant.

In almost all experiments that investigate the heat transfer in ensembles of spherical particles, the heat transfer process is an unsteady conjugate one. For metallic particles, the conductivity ratio takes value considerably greater than 1 and $\Xi >> 1$ (if the fluid is gas) or $\Xi \approx 1$ (if the fluid is liquid). These situations were depicted in Figs. 3 and 4 by the curves $Z_p = 1$ and ($\Phi = \infty$, $\Xi = 1$), respectively. For ceramic, glass and plastic particles, $\Phi \approx 1$ and the volume heat capacity ratio takes values greater than 0.1. These cases are represented in Figs. 3 and 4 by the curves corresponding to $\Phi = 1$ and different Ξ values. Thus, for usual materials, the experimental data are expected to fall (approximately) inside the area limited by the curves plotted in Figs. 3 and 4. In [51] the experimental values of the *Nu* number are smaller than the model predictions. For $Re < 50$, a similar situation can be viewed in Table 7.

The heat transfer rate in ensemble of spherical particles depends on *Re*, *Pr*, ε and the physical properties of the materials. This dependence is complex and cannot be approximated by a single correlation. Similar analysis should be performed with the new developed hydrodynamic models [73–75].

Table 5
Steady *Nu* values for spheres with constant temperature at $Pe = 100$.

γ	ε	*Nu*				
		Creeping	$Re = 0.1$	$Re = 1$	$Re = 10$	$Re = 50$
1.168	0.372	16.81[a]	16.81	16.81	16.81	16.87
		16.94[b]	16.94	16.94	16.94	16.98
1.25	0.488	13.51	13.51	13.51	13.53	13.66
		13.70	13.70	13.70	13.72	13.85
1.5	0.704	9.96	9.96	9.96	9.998	10.34
		10.22	10.22	10.22	10.25	10.60
2	0.875	7.89	7.89	7.89	8.03	8.64
		8.14	8.14	8.15	8.26	8.85
3	0.963	6.76	6.76	6.77	7.10	7.85
		6.95	6.95	6.96	7.23	7.95
∞	1	5.611	5.638	5.805	6.469	7.271

[a] Happel model.
[b] Kubawara model.

Table 6
Steady *Nu* values for spheres with constant temperature at $Pe = 1000$.

γ	ε	*Nu*				
		Creeping	$Re = 0.1$	$Re = 1$	$Re = 10$	$Re = 50$
1.168	0.372	35.38[a]	35.38	35.38	35.39	35.70
		35.98[b]	35.98	35.98	35.997	36.28
1.25	0.488	28.57	28.57	28.57	28.61	29.11
		29.24	29.24	29.24	29.27	29.79
1.5	0.704	20.53	20.53	20.54	20.64	21.69
		21.25	21.25	21.25	21.35	22.38
2	0.875	15.88	15.88	15.89	16.23	17.81
		16.52	16.52	16.52	16.81	18.29
3	0.963	13.38	13.38	13.40	14.17	15.90
		13.83	13.83	13.84	14.47	16.11
∞	1	10.876	10.935	11.302	12.748	14.499

[a] Happel model.
[b] Kubawara model.

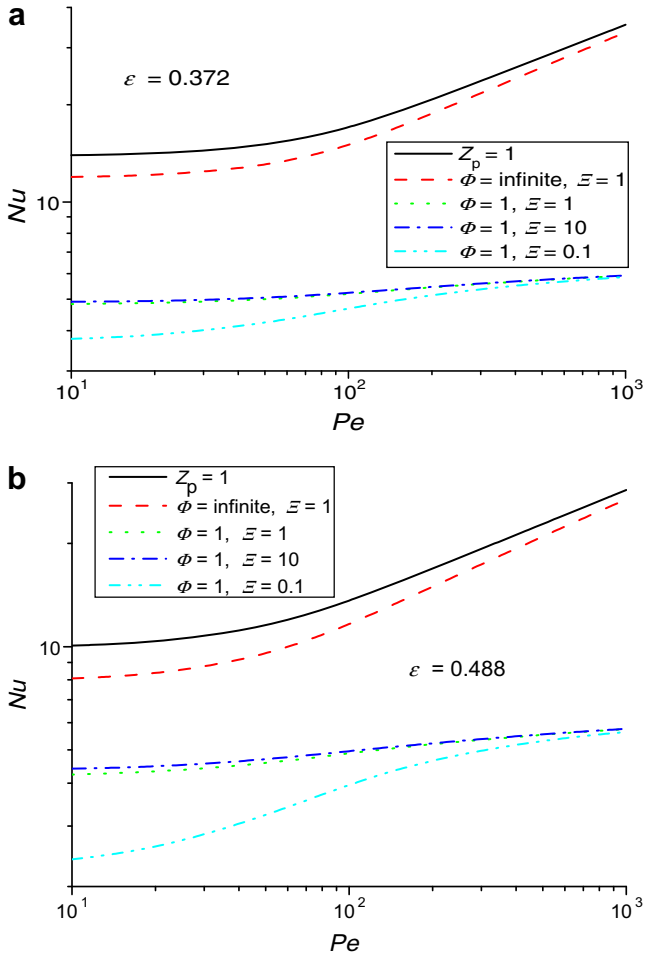

Fig. 3. Asymptotic overall *Nu* number vs. *Pe*; (a) $\varepsilon = 0.372$; (b) $\varepsilon = 0.488$.

5. Conclusions

The numerical results obtained in this work may be summarized as follows (the next statements are valid for the parameters values used in this work, i.e. $Re < 100$ and $10 \leqslant Pe \leqslant 1000$):

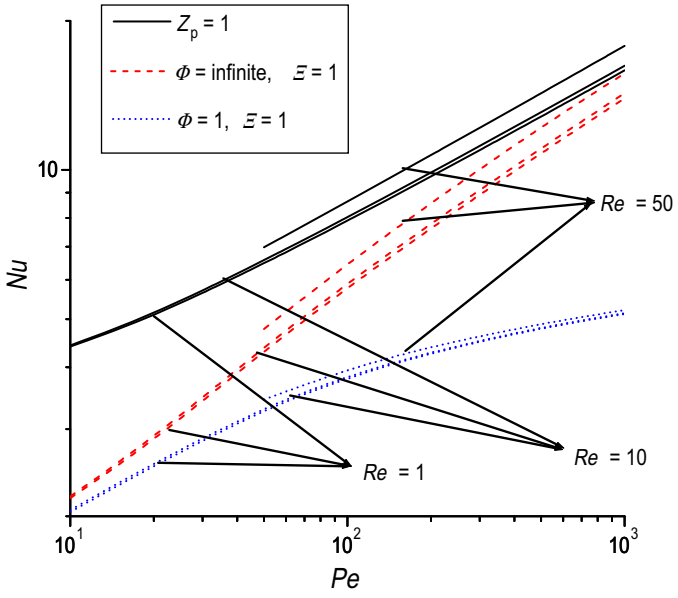

Fig. 4. Asymptotic overall *Nu* number vs. *Pe* for $\varepsilon = 0.875$.

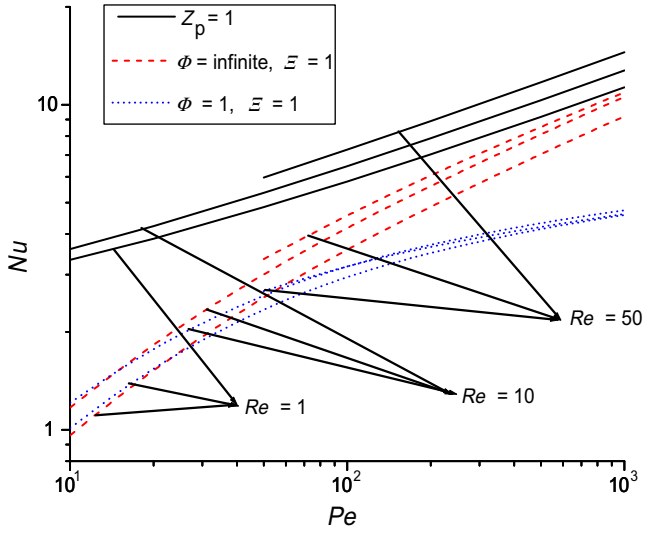

Fig. 5. Asymptotic overall *Nu* number vs. *Pe* for single sphere.

Table 7
Comparison of the present *Nu* values for spheres with constant temperature with published experimental correlations; $\varepsilon = 0.488$.

Re	*Pr*	*Nu* [72]	*Nu* – present
0.1	100	5.65	10.07[a]
			10.08[b]
	1000	12.18	13.51
			13.70
1	10	4.99	10.07
			10.07
	100	10.75	13.51
			13.70
	1000	23.16	28.57
			29.24
10	1	2.32	10.07
			10.07
	10	11.74	13.53
			13.72
	100	23.29	28.61
			29.27
50	1	11.43	11.40
			11.43
	10	24.63	23.15
			23.65
	100	53.06	49.65
			50.93

[a] Happel model.
[b] Kubawara model.

- for given values of ε, *Re* and *Pr*, the influence of the conductivity and volume heat capacity ratios on the conjugate heat transfer follows the same rules as in the case of the single sphere; for $\Phi \to 0$ the asymptotic *Nu* values (overall and internal) tend to the solution of the internal problem; the solution of the internal problem does not depend on Ξ; for $\Phi \to \infty$ the asymptotic *Nu* values (overall and external) tend to the solutions of the external problem; the solution of the external problem depends strongly on Ξ; the decrease in ε decreases the effect of the volume heat capacity ratio;
- the voidage influences the relation between the overall asymptotic *Nu* and (*Re*,*Pr*); for $\epsilon < 0.7$, one may consider that, for a given *Pe* value, the asymptotic *Nu* values do not depend explicitly on *Re*; they depend only on *Pe*; the dependence *Nu* vs. *Pe* is also influenced by ε; for a given *Pe*, the increase in ε

increases the influence of *Re*; for large voidage values and a given *Pe* number, the influence of *Re* on the asymptotic overall *Nu* values is similar but not identical with that of the single sphere; the dependence *Nu* vs. *Re* and *Pe* is also influenced by ε;

– the Happel and Kubawara models provide almost identical heat transfer results.

References

[1] Y.L. Perelman, On conjugate problems of heat transfer, Int. J. Heat Mass Transfer 3 (1961) 293–303.
[2] E. Ruckenstein, Mass transfer between a single drop and a continuous phase, Int. J. Heat Mass Transfer 10 (1967) 1785–1792.
[3] S. Winnikow, The heat and mass transfer from a fluid sphere at large Reynolds and Peclet numbers, Canad. J. Chem. Eng. 46 (1968) 217–222.
[4] B.T. Chao, Transient heat and mass transfer to a translating droplet, J. Heat Transfer 91 (1969) 273–281.
[5] A.V. Luikov, V.A. Aleksashenko, A.A. Aleksashenko, Analytical methods of solution of conjugate problems in convective heat transfer, Int. J. Heat Mass Transfer 14 (1971) 1047–1056.
[6] A.V. Luikov, Conjugate convective heat transfer problems, Int. J. Heat Mass Transfer 17 (1974) 257–265.
[7] I. Pop, D.B. Ingham, A note on conjugate forced convection boundary-layer flow past a flat plate, Int. J. Heat Mass Transfer 36 (1993) 3873–3876.
[8] K.D. Cole, Conjugate heat transfer from a small heated strip, Int. J. Heat Mass Transfer 40 (1997) 2709–2719.
[9] A. Pozzi, R. Tognaccini, Time singularities in conjugated thermo-fluid-dynamic phenomena, J. Fluid Mech. 538 (2005) 361–376.
[10] A. Pozzi, G. Quaranta, R. Tognaccini, A self-similar unsteady flow with conjugated heat transfer, Int. J. Heat Mass Transfer 51 (2008) 1804–1809.
[11] M.A. Antar, A.A. Al-Farayedhi, M.A.I. El-Shaarawi, Steady and transient liquid sphere heating in a convective gas stream, Heat Mass Transfer (Wärme und Stoffübertragung) 36 (2000) 147–158.
[12] A.R. Uribe-Ramirez, W.J. Korchinsky, Fundamental theory for prediction of single-component mass transfer in liquid drops at intermediate Reynolds numbers ($10 \leqslant Re \leqslant 250$), Chem. Eng. Sci. 55 (2000) 3305–3318.
[13] T. Elperin, A. Fominykh, Conjugate mass transfer during gas absorption by falling liquid droplet with internal circulation, Atmos. Environ. 39 (2005) 4575–4582.
[14] B.I. Brounshtein, A.S. Zheleznyak, G.A. Fishbein, Heat and mass transfer in interaction of spherical drops and gas bubbles with a liquid flow, Int. J. Heat Mass Transfer 13 (1970) 963–973.
[15] U.J. Plöcher, H. Schmidt-Traub, Instationärer stofftransport zwischen einer einzelkugel und einer ruhenden umgebung, Chem. Ing. Tech. 44 (1972) 313–319.
[16] F. Cooper, Heat transport from a sphere to an infinite medium, Int. J. Heat Mass Transfer 20 (1977) 991–993.
[17] J. Schirrmann, Unsteady-state mass transfer by fluid particles of changing volume, Int. J. Heat Mass Transfer 33 (1990) 253–266.
[18] L.S. Kleinman, X.B. Reed Jr., Interphase mass transfer from bubbles, drops and solid spheres: diffusional transport enhanced by external chemical reaction, Ind. Eng. Chem. Res. 34 (1995) 3621–3631.
[19] W.H. Chen, An analysis of gas absorption by a liquid aerosol in a stationary environment, Atmos. Environ. 36 (2002) 3671–3683.
[20] H. Brauer, Instationärer Wärmetransport durch die Grenzfläche von Kugeln, Heat Mass Transfer (Wärme und Stoffübertragung) 12 (1979) 145–156.
[21] B. Abramzon, I. Borde, Conjugate unsteady heat transfer from a droplet in creeping flow, AIChE J. 26 (1980) 536–544.
[22] L.B. Baboolal, H.R. Pruppacher, J.H. Topalian, A sensitivity study of a theoretical model of SO_2 scavenging by water drops in air, J. Atmos. Sci. 38 (1981) 856–870.
[23] D.L.R. Oliver, J.N. Chung, Conjugate unsteady heat transfer from a spherical droplet at low Reynolds numbers, Int. J. Heat Mass Transfer 29 (1986) 879–887.
[24] Gh. Juncu, R. Mihail, The effect of diffusivities ratio on conjugate mass transfer from a droplet, Int. J. Heat Mass Transfer 30 (1987) 1223–1226.
[25] D.L.R. Oliver, J.N. Chung, Unsteady conjugate heat transfer from a translating fluid sphere at moderate Reynolds numbers, Int. J. Heat Mass Transfer 33 (1990) 401–408.
[26] H.D. Nguyen, J.N. Chung, Conjugate heat transfer from a translating drop in an electric field at low Peclet number, Int. J. Heat Mass Transfer 35 (1992) 443–456.
[27] H.D. Nguyen, S. Paik, J.N. Chung, Unsteady mixed convection heat transfer from a solid sphere: the conjugate problem, Int. J. Heat Mass Transfer 36 (1993) 4443–4453.
[28] H.D. Nguyen, S. Paik, J.N. Chung, Unsteady conjugate heat transfer associated with a translating spherical droplet: a direct numerical simulation, Numer. Heat Transfer A 24 (1993) 161–180.
[29] H.D. Nguyen, S. Paik, J.N. Chung, Transient conjugated heat transfer analysis from a sphere, Heat Mass Transfer (Wärme und Stoffübertragung) 29 (1994) 431–439.
[30] Gh. Juncu, Conjugate unsteady heat transfer from a sphere in Stokes flow, Chem. Eng. Sci. 52 (1997) 2845–2848.
[31] Gh. Juncu, Unsteady conjugate heat transfer for a single particle and in multiparticle systems at low Reynolds numbers, Int. J. Heat Mass Transfer 41 (1998) 529–536.
[32] Gh. Juncu, The influence of the physical properties ratios on the conjugate heat transfer from a drop, Heat Mass Transfer (Wärme und Stoffübertragung) 35 (1999) 251–257.
[33] Gh. Juncu, The influence of the Henry number on the conjugate mass transfer from a sphere: I – Physical mass transfer, Heat Mass Transfer (Wärme und Stoffübertragung) 37 (2001) 519–530.
[34] S. Paik, H.D. Nguyen, I. Pop, Transient conjugate mixed convection from a sphere in a porous medium saturated with cold pure or saline water, Heat Mass Transfer (Wärme und Stoffübertragung) 34 (1998) 237–245.
[35] L.S. Oliveira, K. Haghighi, Conjugate heat and mass transfer in convective drying of multiparticle systems. Part I: Theoretical considerations, Drying Techn. 16 (1998) 433–461.
[36] H. Amokrane, B. Caussade, Gas absorption into a moving spheroidal water drop, J. Atmos. Sci. 56 (1999) 1808–1829.
[37] A.R. Paschedag, W.H. Piarah, M. Kraume, Numerical simulation of mass transfer between a single drop and an ambiental flow, AIChE J. 47 (2001) 1701–1703.
[38] J. Petera, L.R. Weatherley, Modelling of mass transfer from falling droplets, Chem. Eng. Sci. 56 (2001) 4929–4947.
[39] M.A. Waheed, M. Henschke, A. Pfennig, Mass transfer by free and forced convection from single spherical liquid drops, Int. J. Heat Mass Transfer 45 (2002) 4507–4514.
[40] X. Li, Z.S. Mao, W. Fei, Effects of surface-active agents on mass transfer of a solute into single buoyancy driven drops in solvent extraction systems, Chem. Eng. Sci. 58 (2003) 3793–3806.
[41] W.H. Chen, Atmospheric ammonia scavenging mechanisms around a liquid droplet in convective flow, Atmos. Environ. 38 (2004) 1107–1116.
[42] A.R. Paschedag, W.H. Piarah, M. Kraume, Sensitivity study for the mass transfer at a single droplet, Int. J. Heat Mass Transfer 48 (2005) 3402–3410.
[43] L.S. Kleinman, X.B. Reed Jr., Unsteady conjugate mass transfer between a single droplet and an ambient flow with external chemical reaction, Ind. Eng. Chem. Res. 35 (1996) 2875–2888.
[44] Gh. Juncu, Conjugate heat and mass transfer from a solid sphere in the presence of a nonisothermal chemical reaction, Ind. Eng. Chem. Res. 37 (1998) 1112–1121.
[45] Gh. Juncu, The influence of the Henry number on the conjugate mass transfer from a sphere: II – Mass transfer accompanied by a first-order chemical reaction, Heat Mass Transfer (Wärme und Stoffübertragung) 38 (2002) 523–534.
[46] Gh. Juncu, Conjugate mass transfer to a spherical drop accompanied by a second order chemical reaction inside the drop, Int. J. Heat Mass Transfer 45 (2002) 3817–3829.
[47] Gh. Juncu, Unsteady conjugate mass transfer to a sphere accompanied by a consecutive second-order chemical reaction inside the sphere, Chem. Eng. Process. 45 (2006) 22–30.
[48] S. Burghoff, E.Y. Kenig, A CFD model for mass transfer and interfacial phenomena on single droplets, A.I.Ch.E. J. 52 (2006) 4071–4078.
[49] R. Pfeffer, J. Happel, An analytical study of heat and mass transfer in multiparticle systems at low Reynolds numbers, A.I.Ch.E. J. 10 (1964) 605–611.
[50] R. Pfeffer, Heat and mass transport in multiparticle systems, Ind. Eng. Chem. Fundam. 3 (1964) 380–383.
[51] M.M. El-Kaissy, G.M. Homsy, A theoretical study of pressure drop and transport in packed beds at intermediate Reynolds numbers, Ind. Eng. Chem. Fundam. 12 (1973) 82–90.
[52] Y. Nishimura, T. Ishii, An analysis of transport phenomena of multi-solid particle systems at higher Reynolds numbers by a standard Karman–Pohlhausen method. II Mass Transfer, Chem. Eng. Sci. 35 (1980) 1205–1209.
[53] Z.S. Mao, Y. Wang, Numerical simulation of mass transfer of a spherical particle assemblage with the cell model, Powder Tech. 134 (2003) 145–155.
[54] R. Shukla, S.D. Dhole, R.P. Chhabra, V. Eswaran, Convective heat transfer for power law fluids in packed and fluidized beds of spheres, Chem. Eng. Sci. 59 (2004) 645–659.
[55] F.A. Coutelieris, M.E. Kainourgiakis, A.K. Stubos, Low to moderate Peclet mass transport in assemblages of spherical particles for a realistic adsorption–reaction–desorption mechanism, Powder Tech. 159 (2005) 173–179.
[56] Z.S. Mao, C. Yang, Y. Wang, Effectiveness factor of a catalytic sphere in particle assemblage approached with a cell model, Chem. Eng. Sci. 62 (2007) 6475–6485.
[57] J. Happel, Viscous flow in multiparticle systems: Slow motion of fluids relative to beds of spherical particles, AIChE J. 4 (1958) 197–201.
[58] S. Kubawara, The forces experienced by randomly distributed parallel circular cylinders or spheres in a viscous flow at small Reynolds numbers, J. Phys. Soc. Jpn. (1959) 527–532.
[59] Gh. Juncu, R. Mihail, Numerical solution of the steady incompressible Navier–Stokes equations for the flow past a sphere by a multigrid defect correction technique, Int. J. Numer. Meth. Fluids 11 (1990) 379–395.
[60] Gh. Juncu, A numerical study of steady viscous flow past a fluid sphere, Int. J. Heat Fluid Flow 20 (1999) 414–421.
[61] I. Müller, Thermodynamics and statistical mechanics of fluids and mixtures of fluids, Lecture Notes of the CNR Scuola Estiva della Fisica Matematica, Bari, Cassano, 1976.

[62] A.A. Samarskii, P.N. Vabishchevich, Computational Heat Transfer, Wiley, New York, 1995.
[63] O.A. Ladyzhenskaya, N.N. Ural'tseva, Linear and Quasi-Linear Elliptic Equations, Academic Press, New York, 1968.
[64] J.T. Oden, J.N. Reddy, An Introduction to the Mathematical Theory of Finite Element, Wiley, Baltimore, 1976.
[65] A.A. Samarskii, V.B. Andreev, Méthodes aux Différences pour Equations Elliptiques, Mir, Moscou, 1978.
[66] S.V. Patankar, Numerical Heat Transfer and Fluid Flow, McGraw - Hill, New York, 1980.
[67] P.W. Hemker, A numerical study of stiff two-point boundary problems, Ph.D. Thesis, Mathematisch Centrum, Amsterdam, 1977.
[68] A.K. Jaiswal, T. Sundararajan, R.P. Chhabra, Hydrodynamics of Newtonian fluid flow through assemblages of rigid spherical particles in intermediate Reynolds number regime, Int. J. Eng. Sci. 29 (1991) 693–708.
[69] S.D. Dhole, R.P. Chhabra, W. Eswaran, Power law fluid flow through beds of spheres at intermediate Reynolds numbers Pressure in fixed and distended beds, Chem. Eng. Res. Des. 82 (2004) 642–652.
[70] Z.-G. Feng, E.E. Michaelides, A numerical study on the transient heat transfer from sphere at high Reynolds and Peclet numbers, Int. J. Heat Mass Transfer 43 (2000) 219–229.
[71] Z.-G. Feng, E.E. Michaelides, Heat and mass transfer coefficients of viscous spheres, Int. J. Heat Mass Transfer 44 (2001) 4445–4454.
[72] P.N. Dwivedi, S.N. Upadhyay, Particle–fluid mass transfer in fixed and fluidized beds, Ind. Eng. Chem. Process Des. Dev. 16 (1977) 157–165.
[73] J. Comiti, M. Renaud, A new model for determining mean structure parameters of fixed beds from pressure drop measurements: application to beds packed with parallelepipedal particles, Chem. Eng. Sci. 44 (1989) 1539–1545.
[74] R. di Felice, The particle-in-a-tube analogy for a multiparticle suspension, Int. J. Multiphase Flow 22 (1996) 515–525.
[75] E. Mauret, M. Renaud, Transport phenomena in multi-particle systems – II. Proposed new model based on flow around submerged objects for sphere and fiber beds – transition between the capillary and particulate representations, Chem. Eng. Sci. 52 (1997) 1819–1834.